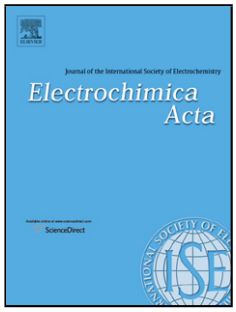

Title: Photoinduced charge separation in organic-inorganic hybrid system: C_{60}-containing electropolymer / CdSe-quantum dots

Author: Manuel Otero Thomas Dittrich Jörg Rappich Daniel A. Heredia Fernando Fungo Edgardo Durantini Luis Otero

PII: S0013-4686(15)01141-X
DOI: http://dx.doi.org/doi:10.1016/j.electacta.2015.05.029
Reference: EA 24962

To appear in: *Electrochimica Acta*

Received date: 4-2-2015
Revised date: 6-4-2015
Accepted date: 6-5-2015

Please cite this article as: Manuel Otero, Thomas Dittrich, Jörg Rappich, Daniel A.Heredia, Fernando Fungo, Edgardo Durantini, Luis Otero, Photoinduced charge separation in organic-inorganic hybrid system: C60-containing electropolymer / CdSe-quantum dots, Electrochimica Acta http://dx.doi.org/10.1016/j.electacta.2015.05.029

Photoinduced charge separation in organic-inorganic hybrid system: C_{60}-containing electropolymer / CdSe-quantum dots

Manuel Otero[‡] and Thomas Dittrich.

Helmholtz Center Berlin for Materials and Energy, Institute of Heterogeneous Materials, Hahn-Meitner-Platz 1, D-14109 Berlin, Germany.

Jörg Rappich

Helmholtz Center Berlin for Materials and Energy, Institute of Silicon Photovoltaics, Kekuléstr. 5, D-12489 Berlin, Germany

Daniel A. Heredia, Fernando Fungo, Edgardo Durantini and Luis Otero*

Departamento de Química, Universidad Nacional de Río Cuarto, Agencia Postal N^{o} 3, X5804BYA, Río Cuarto, Argentina.

*Corresponding author
e-mail: lotero@exa.unrc.edu.ar
Phone: +543584676111
Fax: +543584676233

[‡] Present address: INFIQC, Departamento de Matemática y Física, Facultad de Ciencias Químicas, Universidad Nacional de Córdoba, Ciudad Universitaria, 5000 Córdoba, Argentina.

Graphical Abstract

Highlights

- Modified ethylenedioxythiophene allows the formation of an electropolymer holding C_{60}.
- Polymer decoration with CdSe QDs produces a photoactive organic-inorganic interface.
- Photoinduced electron transfers were analyzed by surface photovoltage.
- The interface is a potential structure for the development of optoelectronic devices.

Abstract

A photoactive interface is formed between an electrochemical generated organic polymer film and CdSe quantum dots. The specifically designed and synthesized 3,4 ethylenedioxythiophene electroactive monomer, holding C_{60} buckminsterfullerene, allows the formation of thin films containing both, electron acceptor and hole transport moieties. The generation of photoinduced heterogeneous charge transfer in CdSe quantum dots-electropolymer system was characterized by time resolved and spectral dependent surface photovoltage. In films containing C_{60} moieties whose surface was modified with 5 nm CdSe quantum dots, the illumination generated photovoltage values around twenty times larger than those obtained without nanoparticles decoration. The results show that

this organic-inorganic hybrid interface is a potential structure for the development of optoelectronic devices.

Keywords: Polyethylenedioxythiophene-C_{60}; Electro-polymerization; Organic-inorganic hybrid systems; CdSe quantum dots.

1. Introduction

The continuous growing of energy demands around the world and the environmental pollution resulting in global warming have led to a greater focus of research in renewable energy sources over the past decades.[1,2] Contrary to the fossil fuels, solar energy is available profusely in most of the world regions. Thus, the development of economically competitive technology in solar energy conversion is nowadays of vital importance.

In this context, organic based photovoltaic devices have introduced the potential of obtaining cheap and easy methods to produce energy from light [1,3-6]. Organic semiconductors have several advantages such as low-cost synthesis, and easy manufacture of thin film devices by different methodologies (spin-coating, layer by layer deposition, electrosynthesis, deep coating) [7-10]. Thus, organic solar cells (OSC) are one of the most promising energy conversion devices, and for this reason a large amount of research has been carried out in this field [1,3-6]. However, although organic materials used in solar cells exhibit low fabrication

costs and the possibility to use flexible substrates, they still show low energy conversion efficiency [1,11].

One of the limitations in the improvement of OSC is the mobility of charge carriers, which is lower than in inorganic semiconductors [12], allowing a deleterious recombination process. A possible solution to this problem could be the use of composite hybrid materials formed by organic polymers and inorganic semiconductors, where photoinduced charge transfer and carrier transport processes are possible [12-16].

In addition, nanotechnology holds a significant potential for the development of new systems capable to overcome the mentioned limitations. Colloidal semiconductor nanocrystals (NCs) possess unique properties determined by the confinement of charge carriers within a restricted volume [17] and have been used as components of photovoltaic devices [18-22]. Moreover, they can be designed and synthesized with the desirable characteristics to improve their electric and optic properties. One of the most used materials employed in hybrid solar cells are CdSe quantum dots (QDs) [23-27 which can be modified in their band-gap altering their size and shape, producing materials able to absorb in a wide range of the visible spectrum.

On the other hand, a promising technique to produce optoelectric active conducting polymer films is the electropolymerization with the use of electroactive monomers. Polymerization through electrochemical deposition techniques allows the synthesis of organic polymers in one step, with suitable control over film formation [7-9,28-29]. A number of reports revealed that the polymeric films

obtained electrochemically over conductive solid substrates are highly stable, showing compact layers, with excellent stuck to the electrode, high charge transport capability and adequate optical properties [7-9,28-31 These features are key parameters in the manufacture of organic optoelectronic devices. However, until now, only a few number of studies showed real application of the electrochemical film deposition methodology in the generation optoelectronic devices [8,28,29,32,33].

The purpose of this work is to examine the photoinduced charge separation processes in CdSe QDs deposited on electropolymer films containing C_{60} buckminsterfullerene as electron acceptor group. This organic polymer is obtained from a specifically designed electroactive monomer formed by 3,4-ethylenedioxythiophene (EDOT) holding C_{60} moieties (EDOT-C_{60}, Figure 1). We demonstrated, using surface photovoltage spectroscopy (SPV) [34], the capacity of this system for the generation of photoinduced charge separated states. This fact turns the material into a potential structure for to apply in the design and development of optoelectronic devices. Little research has been conducted in relation to this field of study, and this article provides one of the few examples of using SPV to study the charge separation in these hybrid systems [35-36].

2. Experimental

2.1. Synthesis and Characterization of EDOT-C_{60} monomer.

2-((4-Bromobutoxy)methyl)-2,3-dihydrothieno[3,4-b][1,4]dioxine (1).- A solution of (2,3-dihydrothieno[3,4-*b*][1,4]dioxin-2-yl)methanol (100 mg, 0.58 mmol),

1,4-dibromobutane (1 mL, 8.3 mmol) and tetrabutylammonium bromide (TBAB, 56 mg, 0.17 mmol) in 2.5 mL of dichloromethane (DCM) was stirred for 5 min. After that, a solution of NaOH (2.5 mL, 50 % w/w) was added and the reaction was stirred at room temperature for 2 h. The reaction mixture was diluted with 50 mL water and then extracted with DCM. The solvent was removed under reduced pressure and the residue was subjected to flash column chromatography (silica gel, DCM) affording **1** (167 mg, 94 %), as a white solid. R_f (silica gel, DCM)= 0.6. ^{1}H NMR ($CDCl_3$, TMS) δ [ppm]: 6.34 (d, *J* = 3.8 Hz, 1H), 6.32 (d, *J* = 3.8 Hz, 1H), 4.26 – 4.33 (m, 1H), 4.23 (dd, *J* = 11.6 Hz, 2.2 Hz, 1H), 4.05 (dd, *J* = 11.6 Hz, 7.4 Hz, 1H), 3.69 (dd, *J* = 10.4 Hz, 5.0 Hz, 1H), 3.61 (dd, *J* = 10.4 Hz, 5.8 Hz, 1H), 3.54 (t, *J* = 6.7 Hz, 2H), 3.44 (t, *J* = 6.7 Hz, 2H), 1.95 (q, *J* = 6.7 2H), 1.74 (q, *J* = 6.7, 2H). ^{13}C NMR ($CDCl_3$) δ [ppm] = 141.6, 141.6, 99.8, 99.7, 72.7, 71.0, 69.3, 66.2, 33.7, 29.6, 28.2. MS [*m/z*] 306 (M^+); $C_{11}H_{15}BrO_3S$ requires *m/z* 305.99. FT-IR (KBr) ν [cm^{-1}]: 2939, 2870, 1579, 1487, 1375, 1184, 1124, 1020, 858, 756.

2-((4-Azidobutoxy)methyl)-2,3-dihydrothieno[3,4-b][1,4]dioxine (2). Compound **1** (307 mg, 1 mmol) was dissolved in DMF (10 mL) and NaN_3 (975 mg, 15 mmol) was added. The reaction mixture was stirred at 85 °C for 12 h under Ar in the absence of light. Then, water (30 mL) and DCM (30 mL) were added. The organic phase was extracted and the solvent were evaporated under reduced pressure to afford **2** (267 mg, 995), as a yellow oil. R_f (silica gel, DCM)= 0.4. ^{1}H NMR ($CDCl_3$, TMS) δ [ppm]: 6.33 (d, *J* = 3.7 Hz, 1H), 6.32 (d, *J* = 3.7 Hz, 1H), 4.26 – 4.33 (m, 1H), 4.23 (dd, *J* = 11.6 Hz, 2.2 Hz, 1H), 4.05 (dd, *J* = 11.6 Hz, 7.4 Hz, 1H), 3.69 (dd, *J* = 10.4 Hz, 5.0 Hz, 1H), 3.60 (dd, *J* = 10.4 Hz, 5.7 Hz, 1H), 3.53 (t,

J = 5.8 Hz, 2H), 3.30 (t, *J* = 6.3 Hz, 2H), 1.67 (q, *J* = 3.1, 4H). ^{13}CNMR ($CDCl_3$) δ [ppm] = 141.6, 141.6, 99.8, 99.7, 72.7, 71.3, 69.3, 66.2, 51.3, 26.8, 25.8. MS [*m/z*] 269 (M^+); $C_{11}H_{15}N_3O_3S$ requires *m/z* 269.08. FT-IR (NaCl) ν [cm^{-1}]: 2935, 2920, 2870, 2096, 1676, 1487, 1375, 1253, 1186, 1126, 1087, 1020, 858, 761.

Preparation of the EDOT-C_{60} monomer. A mixture of C_{60} (198 mg, 0.27 mmol) and **2** (64 mg, 0.24 mmol) was dissolved in dry *o*-dichlorobenzene (*o*-DCB, 50 mL). The solution was heated under reflux for 78 h under Ar atmosphere in the absence of light. The solvent was evaporated under vacuum and the dark residue was purified by flash column chromatography (silica gel, toluene/hexane, 5:1) to afford EDOT-C_{60} (103 mg, 45%), as a dark brown powder. R_f (silica gel, toluene)= 0.75. ^{1}H NMR ($CDCl_3$, TMS) δ [ppm]: 6.35 (d, *J* = 3.6 Hz, 1H), 6.33 (d, *J* = 3.6 Hz, 1H), 4.31 – 4.41 (m, 1H), 4.28 (dd, *J* = 11.6 Hz, 2.0 Hz, 1H), 4.11 (dd, *J* = 11.6 Hz, 7.4 Hz, 1H), 3.65 – 3.88 (m, 6H), 1.95 – 2.18 (m, 4H). ^{13}CNMR ($CDCl_3$) δ [ppm] = 147.8, 146.7, 145.0, 144.7, 144.5, 144.4, 144.3, 144.1, 143.8, 143.6, 143.4, 143.2, 143.1, 142.9, 142.8, 142.7, 141.5, 141.4, 140.7, 139.3, 139.2, 138.5, 138.0, 137.8, 137.3, 137.2, 136.2, 135.8, 133.7, 99.7, 99.6, 72.7, 71.6, 69.3, 66.2, 51.4, 27.3, 26.2, 14.1. ESI-MS [*m/z*] 962.0851 [$(M+H)^+$]; $C_{71}H_{15}NO_3S$ requires *m/z* 961.0773. FT-IR (KBr) ν [cm^{-1}]: 2918, 2850, 2362, 2331, 1481, 1423, 1363, 1340, 1180, 1124, 1022, 858, 744, 524.

Proton nuclear magnetic resonance spectra were performed on a FT-NMR Bruker Avance 300 spectrometer. ^{1}H and ^{13}CNMR spectra were acquired at 300.13 and 75.48 MHz, respectively. Mass Spectra were recorded on a Bruker micrOTOF-QII (Bruker Daltonics, MA, USA). FT-IR spectra were recorded on a Shimadzu

Prestige 21 spectrophotometer. All chemicals were acquired from Aldrich and used as received.

2.2. Electrochemistry and Photoelectrochemistry.

Cyclic Voltammetry. Electrochemical characterization of EDOT-C_{60} was carried out in 1 mM *o*-DCB solution containing 0.1 M tetrabutylammonium tetrafluoroborate (TBATFB). A gold disk was used as working electrode. The cyclic voltammetry (CV) experiments were carried out in a three electrodes cell configuration using an Ag/AgCl (KCl sat.) reference electrode and a large area Pt foil as a counter electrode. All the measurements were conducted at room temperature using a potentiostat-galvanostat Autolab (Electrochemical Instruments). Electrochemical polymerization was carried out also over semitransparent indium tin oxide (ITO) electrodes (Delta Technologies nominal resistance of 8–12 Ω/square) by the same procedure. Ethylenedioxythiophene (EDOT) and (2,3-dihydrothieno[3,4-*b*][1,4]dioxin-2-yl)methanol (EDOT-OH) electro-polymerization to form poly-ethylenedioxythiophene (PEDOT) and poly-(2,3-dihydrothieno[3,4-*b*][1,4]dioxin-2-yl)methanol (PEDOT-OH) respectively were carried out using the same electrochemical set-up in dichloromethane containing 0.1 M tetrabutylammonium hexafluorphosphate (TBAHFP). For SPV experiments, the film formation by electro-polymerization was carried out on large area Au electrodes obtained by evaporation on glass coated with Cr as adhesion layer. Before use, gold substrates were cleaned for 15 min in an ultrasonic bath containing isopropanol, rinsed with water and submerged in a solution of hydrogen

peroxide and sulfuric acid (piranha solution) for 30 seconds in order to remove organic residues. Finally, the electro-deposited layers were washed with ultrapure water and dried under a nitrogen stream. For comparison, some PEDOT films were prepared under similar conditions as for the PEDOT-C_{60} films.

Surface photovoltage. The light-induced change of the contact potential difference is measured by SPV techniques. SPV signals are sensitive to the amount of photo-generated charge and to the distance between the centers of positive and negative charge distributions. Here, modulated and transient SPV signals were measured in the arrangement with a fixed capacitor.

The measurements of modulated SPV were performed with chopped light (modulation frequency 8 Hz) from a quartz prism monochromator (SPM2) and a halogen lamp (100 W). The SPV signals were detected with a high impedance buffer (measurement resistance 10 GΩ). The measurements were carried out in vacuum. The SPV spectra were not normalized to the photon flux. The sign of the in-phase SPV signal is positive (negative) if the photo-generated electrons are preferentially separated towards the internal (external) surface. The absolute value of the in-phase signal is in maximum and the phase-shifted by 90° signal is zero, i.e. the phase angle is 0 or ~180°, if the time constants of the increasing and decreasing signals are much shorter than the modulation period. SPV transients were excited in the absorption maximum of the first excitonic transition of the given CdSe-QDs with laser pulses (wavelength 590 nm, time of laser pulses: 5 ns, intensity: about 3 mJ/cm²) and recorded with a sampling oscilloscope (GAGE compuscope CS 14200) at resolution of 10 ns.

2.3. Decoration of electro-polymerized PEDOT-C_{60} films with CdSe-QDs

Pyridine end-capped CdSe-QDs (4.5 nm diameter, onset absorption ~ 1.9 eV, Bayer Technology Services GmbH) were deposited onto electropolymer films by dipping from diluted QD suspension (5 mg/g in pyridine). The withdrawal speed (1 mm/s) of the samples was controlled with a robot leaving a layer of CdSe-QDs on the substrate [for detailed procedure see reference 37]. EDOT-C_{60} electropolymer films (PEDOT-C_{60}) characterization was performed by scanning electron microscopy (SEM) on a Carl Zeiss EVO MA 10 with electron beam energy of 20 keV. The film thicknesses on gold substrates were measured with a step-profiler (Bruker Dektak 8).

3. Results and Discussion

3.1. EDOT-C_{60} Synthesis Procedure

Details of EDOT-C_{60} synthesis method were depicted in experimental section. Figure 1 shows a diagram of the general procedure. Commercially available hydroxymethyl-EDOT was modified at room temperature through the incorporation of a bifunctional alkyl chain (**1**) which is an aliphatic nucleophilic substitution reaction under phase transfer catalyst (PTC) conditions. This heterogeneous catalysis reaction allowed to achieve faster transformations at room temperature, with a yield increment by suppression of side reactions [38]. After obtaining the bromide **1** in 94 % yield, a second nucleophilic reaction in an aprotic polar solvent (DMF) with sodium azide (NaN_3) afforded **2** in quantitative yield.

Finally, in order to obtain EDOT-C_{60}, a dipolar [1,3]-cycloaddition between **2** and fullerene in dry *o*-DCB was carried out by refluxing in the dark. The mono-addition to the [5,6] bond produced the aza-bridged fulleroids, EDOT-C_{60}, in 45% yield.

The molecular structure of the EDOT-C_{60} monomers was corroborated by FT-IR and NMR spectroscopies. Comparison of the FT-IR spectra of **2** and EDOT-C_{60} clearly revealed the disappearance of the characteristic absorption of the azide moiety, at 2096 cm^{-1} along with the characteristic band of the organo-fullerenes, at 525 cm^{-1} [39]. On the other hand, the ^{1}H-NMR spectrum of EDOT-C_{60} was very similar to that of the starting azide, with a slight downfield shift in the signals of the EDOT group, due to fullerene electron withdrawing effect. Finally, the ^{13}C NMR spectrum of the fullerene derivate showed the characteristic signals of the EDOT ring, between 25 and 130 ppm and all the signals attributable to the C_{60} moiety were observed in the range 130-150 ppm, which corresponds to the sp^2 region of the spectrum. Furthermore, no signals related to an sp^3 hybridization of the carbon atoms in C_{60}, characteristic of a closed [6,6] structure, could be detected (70-90 ppm). These facts clearly indicate that the cycloaddition reaction resulted in the formation of an open [5,6] structure [40,41].

3.2. Electrochemistry and electropolymerization of EDOT-C_{60}.

Cyclic voltammetry in *o*-DCB containing 0.1 M TBATFB as supporting electrolyte was used in order to analyze the redox properties and the stability of radical ions of EDOT-C_{60}. Figure 2(a) shows successive voltammograms of EDOT-C_{60} on gold electrodes. In the first cycle of the anodic scan, an irreversible

oxidation process was detected at ~1.25 V, which can be assigned to the formation of EDOT radical cations [42,43]. In the cathodic sweep, the multiple reversible reduction waves related to the presence of C_{60} moiety was clearly observed [44-47]. These results are in agreement with the structural characteristic of EDOT-C_{60} and probe that the main electronic characteristic of both moieties are retained in this dyad molecule.

In successive potential cycles, the electro-polymerization process is evidenced by the concomitant increment in the current of all redox peaks. Therefore, the electrochemical oxidative polymerization enables the direct growth of polymeric thin films. This is typical for EDOT containing derivatives [48], where the coupling of the radical cations with proton loses leads to the formation of a stable and electroactive film on the electrode surface. Furthermore, when the electrode is removed from the electrochemical cell and transferred to another cell with only electrolyte solution, it shows the redox responses depicted in Figure 2(b). The CV shaped obtained is quite different than those observed for PEDOT modified electrodes. The reversible wide wave observed at - 0.77 V is not present in unsubstituted EDOT polymers. Thus, this wave must be assigned to the redox processes in the C_{60} residues, indicating that, after electro-polymerization of EDOT units, fullerene moieties are retained in the film. However, the typical C_{60} voltammetric waves, observed in the first potential cycles, merge in a unique envelopment wave, with the increase of the amount of deposited material. It is common the observation of the widening and eventual overlapping of the voltammetric peaks in organic polymeric films [49]. This is generally due to the

interaction between the redox centers in the solid state, changes in the solvation and charges diffusion phenomena. This material is going to be referred as PEDOT-C_{60}. Through the same procedure, PEDOT-C_{60} films where obtained on ITO and large area gold electrodes. Figures 3a and 3b show the UV-visible absorption spectrum of EDOT-C_{60} monomer in DCM solution and the diffuse reflectance spectrum of the electropolymerized PEDOT-C_{60} film on ITO, respectively. The monomer shows the typical fullerene transitions at 261 and 332 nm [50,51]. These fact, together with the lack of the band at ~ 420-440 nm attributed to the 6,6 closed structure [50,51], are agreement with the formation of the open 5,6 structure during the EDOT-C_{60} monomer synthesis. On the other hand, the polymer film formation on ITO surface confers a yellow-brownish coloration to the transparent electrode (see inserted picture in Figure 3b). The diffuse reflectance spectrum shows that the buildup of a conjugated system produces a broad absorption starting from ~600 nm, with a shoulder at ~ 520 nm that can be attributed to the π-π^* transition. This value is ~ 90 nm blue-shifted as compared to the reference PEDOT-OH (an electropolymer obtained from the monomer precursor (EDOT-OH), see experimental section) that displays a well-defined band, with a maximum at 610 nm (result not shown). Such a blue-shift, observed also in other structurally related polymers [52], could be originated in the shortening of the effective conjugation length in PEDOT-C_{60}. This effect may be explained by steric hindrance due to the bulkyness of the fullerene substituents. A tridimensional idealized structure obtained by molecular mechanics calculations (MM+ at HyperChem software) of the PEDOT-C_{60} polymer is shown in Figure 4. According to this spatial geometry a

"double cable" polymeric structure can be suggested for the synthetized material, as was already proposed for related molecular structures. [53-55]

The film thicknesses were modified through the control of the number of electro-polymerization cycles. Figure 5 shows a typical cross section of a PEDOT-C_{60} layer electro-deposited on a gold substrate (10 cycles). The electro-deposited PEDOT-C_{60} layer thickness, measured by step profilometry, varied between about 80 and 300 nm. The insert of Figure 5 gives an impression about the homogeneity of the complete electro-deposited PEDOT-C_{60} layer. Figure 6 shows the relationship between the PEDOT-C_{60} film thickness and the number of electro-polymerization cycles analyzed by scanning electron microscopy (SEM) and the height across the PEDOT-C_{60}/Au substrate boundary for 2 and 10 deposition cycles (insert). Slight discrepancies between SEM analysis and step profilometry are probably caused by shrinkage of structures under the electron beam and/or by pick-up of soft polymer material by the needle of the step profiler.

3.3. Time resolved SPV

The surface photovoltage method is a well-known, non-contact technique to measure the photoinduced charge separation, which produces a change in the contact potential difference (CPD) [56-58]. A contact potential difference between the sample surface and a reference is obtained in darkness. However, when the sample is illuminated, the light can induce a change of the charge distribution, which is proportional to the change in the contact potential (ΔCPD). SPV is sensitive to the amount of photoinduced charge carriers separated in space and to

the distance between the centers of positive and negative charge distributions. The capability of a series of electrochemical generated organic films for the generation of light-induced charge separate states was shown by SPV in previous studies [7,59,60].

SPV transients shown in Figure 7 were excited with laser pulses with a photon energy of 2.1 eV being absorbed in the CdSe-QDs (in agreement with the absorption gap of QDs-CdSe [61]) and giving a maximum in the SPV spectra (vide infra). For CdSe-QDs/Au and CdSe-QDs/PEDOT-C_{60}, the SPV signals were positive, i.e. photo-generated electrons were separated from the CdSe-QDs into electronic states at the interface between CdSe-QDs and Au or into C_{60} moieties in the PEDOT-C_{60} electropolymer, respectively. The sign of the SPV signal was negative for CdSe-QDs/PEDOT, i.e. photo-generated electrons were separated towards the CdSe-QDs which is equivalent with the separation of photo-generated holes into PEDOT. In the case of PEDOT-C_{60}/Au the transient signal is indistinguishable from the noise level.

On the other hand, the maximum of the SPV signals in Figure 7 appeared within the duration time of the laser pulse. Therefore, fast charge separation took place in organic-inorganic hybrid structures containing CdSe-QDs. The corresponding mechanisms of fast local charge separation are schematically shown for CdSe-QDs/Au, CdSe-QDs/PEDOT and CdSe-QDs/PEDOT-C_{60} (Figure 8a-c, respectively).

The relaxation of the SPV transients has been fitted with stretched exponentials. Stretched exponential function (Kohlrausch function) is frequently

used for the phenomenological description of relaxation in disordered systems [62]. For the samples CdSe-QDs/Au and CdSe-QDs/PEDOT-C_{60}, excellent fits were obtained by using two stretched exponentials (for a detailed procedure see reference [63]) with not very different stretching parameters of 0.23 (characteristic times 3 and 0.13 ms for CdSe-QDs/Au and CdSe-QDs/PEDOT-C_{60}, respectively) and 0.17 (characteristic time 40 and 1.2 ns for CdSe-QDs/Au and CdSe-QDs/PEDOT-C_{60}, respectively). It is interesting to mention that identical stretching parameters could be used for the fits for both samples whereas the characteristic times were significantly shorter for CdSe-QDs/PEDOT-C_{60}. On the other side, at least four stretched exponentials were required for fitting of the SPV transient of sample CdSe-QDs/PEDOT. Roughly, in the case of CdSe-QDs/PEDOT-C_{60} system, the signal reached 50% of its initial value after about 5 μs, which was about one order of magnitude slower than CdSe-QDs/PEDOT for similar thickness films. This could indicate than C_{60} moiety plays a relevant role as electron acceptor in the generation of photovoltaic effects in the organic-inorganic hybrid system.

The SPV transients of the CdSe-QDs/Au and CdSe-QDs/PEDOT-C_{60} samples were rather similar to those reported on ITO (indium tin oxide) substrates [**Error! Bookmark not defined.**,64]. It has been shown that the relaxation of the SPV transients can be well described by Miller-Abrahams hopping of holes in CdSe-QDs and distance dependent recombination with electrons fixed at the ITO site, whereas a density of about 10 hole-traps per QD at the surface of CdSe-QDs has been found [64]. A similar relaxation mechanism limited by trapping of holes at CdSe-QD surface states might be assumed for the CdSe-QDs/Au and CdSe-

QDs/PEDOT-C_{60} samples. However, one has to keep in mind that the distribution of defect states is affected as well by the dielectric constant and by the work function of the surrounding of a QD. Therefore, on the base of the given experiments, it cannot be distinguished whether trapping of holes or of electrons limit the characteristic times. In addition, transport of holes in PEDOT or of electrons in neighbored C_{60} moities may become important in the case of low mobility. The limiting process or processes cannot be well distinguished for the CdSe-QDs/PEDOT sample since both trapping of electrons at surface states at CdSe-QDs and transport of holes in a chain of the conjugated polymer have to be considered.

3.4. Spectral dependent modulated SPV

Spectral dependent modulated SPV measurements give information about transitions from which charge separation takes place. Figure 9 shows the spectra of in-phase (x-signals) and phase-shifted by 90° (y-signals) SPV signals for CdSe-QDs/Au (a), CdSe-QDs/PEDOT (b), PEDOT-C_{60} (c) and CdSe-QDs/PEDOT-C_{60} (d) samples [note that in order to facilitate the comparison the actual SPV amplitudes are enlarged ten times in (b) and (c) figures, and two times in (a)]. As a remark, the x-signals follow rapidly the modulated light, i.e. the x-signals correspond to electronic states with a relaxation time faster than the modulation period. Similarly, the y-signals correspond to electronic states with a relaxation time longer than the modulation period.

The x-signals and y-signals of the first excitonic peak of the CdSe-QDs/Au sample were positive and negative, respectively (Figure 9a). This corresponded to a preferential separation of photo-generated electrons from the CdSe-QD towards the gold surface, which was in agreement with the SPV transient. The x-signal of the first excitonic peak set on at about 1.95 eV and reached its maximum at about 2.1 eV.

The signs of the x- and y-signals changed for the CdSe-QDs/PEDOT sample what was also in agreement with the SPV transient. Transitions related to absorption in PEDOT and leading to charge separation appeared at photon energies below the first excitonic peak of CdSe-QDs. It should be remarked that PEDOT electropolymer films of similar thickness without QDs decoration do not present surface photovoltage signal.

The signs of the x- and y-signals were similar for the CdSe-QD/Au, PEDOT-C_{60} and CdSe-QDs/PEDOT-C_{60} samples. Interestingly, transitions related to absorption in PEDOT-C_{60} and leading to charge separation in the PEDOT-C_{60} sample disappeared in the CdSe-QDs/PEDOT-C_{60} sample. Therefore, the optical transitions related to absorption in PEDOT-C_{60} (see Figure 3b) and leading to charge separation in the PEDOT-C_{60} sample were related to the near surface region which was strongly influenced by decoration with CdSe-QDs.

It is important to note that when PEDOT-C_{60} film surfaces are modified with 5 nm CdSe quantum dots, the resultant photovoltage value is around twenty times larger than those obtained for PEDOT-C_{60} polymer films of same thickness films (Figure 9). The SPV results in CdSe-QDs/PEDOT-C_{60} system indicate that

photoinduced electron transfer from QDs-CdSe to high electron affinity C_{60} is taken place in the hybrid organic-inorganic material. These evidences are reinforced by the fact that, when QDs-CdSe are deposited on PEDOT electropolymer films, lower SPV signals are observed (Figure 9), with sign inversion, denoting that the photogenerated electrons are preferentially moved to the external surface. Has been demonstrated that the introduction of CdSe quantum dots in bulk heterojunction organic solar cells, holding a C_{60} buckminsterfullerene derivative as electron acceptor, produces a noticeable enhancement in the cell´s power conversion efficiencies [65]. The QDs-CdSe conduction band lays ~ 0.5 eV at higher energy that C_{60} lower unoccupied molecular orbital (LUMO), making photoinduced electron transfer thermodynamically feasible [65]. This mechanism has been proposed as the responsible of photocurrent enhancement in ternary (organic polymer-CdSe-C_{60}) energy conversion devices containing tri-octylphosphine oxide (TOPO) caped CdSe quantum dots [66]. However, electron transfer from organic polymers (ej. poly-3-hexyl thiophene (P3HT) [67,68] and poly[2-methoxy-5-(2'-ethylhexyloxy)-p-phenylene vinylene] (MEH-PPV) [69]) to CdSe quantum dots has been also well documented, which is agreement with inverted surface photovoltage sign that we here reported, between CdSe-QDs/PEDOT and CdSe-QDs/PEDOT-C_{60} samples. These facts demonstrate that the developed material could be used as building block in the construction of hybrid photovoltaic cells based in organic/inorganic nanocomposites [70].

The ratio between the absolute values of the maximum y- and x-signals was about 1.7, 3.4, 5.9 and 14 for the PEDOT-C_{60}, CdSe-QD/Au, CdSe-QDs/PEDOT

and CdSe-QDs/PEDOT-C_{60} samples, respectively. This shows that the response of the modulated SPV signals was much more retarded for the samples containing CdSe-QDs and gives additional evidence for the role of hole traps at the CdSe-QDs. The very strong y-signal of the CdSe-QDs/PEDOT-C_{60} sample seems surprising since the characteristic times obtained from the stretched exponentials were much shorter for this sample than for the CdSe-QD/Au sample. Here, one has to take into account that the measurement conditions are rather different for transient and modulated SPV measurements. In transient SPV measurements, a short laser pulse is used for excitation after a long relaxation time in the dark. In modulated SPV measurements, the time intervals are identical for illumination and dark, i.e. traps can be very differently occupied for transient and modulated SPV determinations.

4. Conclusions

The synthesis of a 3,4 ethylenedioxythiophene holding C_{60} buckminsterfullerene linked by an aliphatic chain allowed the formation of thin films over a gold substrate containing both, the electron acceptor and the hole transport moieties. These films were obtained by electropolymerization, allowing the polymer synthesis and the film deposition in one step, with suitable thickness control. The generation of photoinduced heterogeneous charge transfer between CdSe quantum dots and PEDOT-C_{60} electropolymer was proved by transient and spectral dependent modulated surface photovoltage, demonstrating the potential

applicability of the new organic polymer and the hybrid organic-inorganic material in the building of optoelectronic devices.

Acknowledgments. Authors are grateful to Secretaría de Ciencia y Técnica, Universidad Nacional de Río Cuarto (Secyt-UNRC) and Consejo Nacional de Investigaciones Científicas y Técnicas (CONICET) of Argentina for financial support. This work was supported by the Deutscher Akademischer Austausch Dienst (DAAD) - Ministerio de Ciencia, Tecnología e Innovación Productiva (MinCyT) join project (DA/10/06). D.A.H. and M.O. thank to CONICET and HZB respectively for research fellowships.

5. References

[1] S. B. Darling, F. You. RSC Adv. 3 (2013) 17633.

[2] H. Zhou, Y. Qu, T. Zeid, X. Dua. Energy Environ. Sci. 5 (2012) 6732.

[3] B. Ratier, J-M. Nunzi, M. Aldissi, T.M. Kraft, E. Buncel. Polym. Int. 61 (2012) 342.

[4] S. Günes, H. Neugebauer, N.S. Sariciftci. Chem. Rev. 107 (2007) 13248.

[5] Y-J. Cheng, S-H. Yang, C-S Hsu. Chem. Rev. 109 (2009) 5868.

[6] W. Tang, J. Hai, Y. Dai, Z. Huang, B. Lu, F. Yuan, J. Tang, F. Zhang. Sol. Energy Mater. Sol. Cells. 94 (2010) 1963.

[7] P. Zabel, T. Dittrich, Y-L. Liao, C-Y. Lin, K-T. Wong, F. Fungo, L. Fernandez, L. Otero. Org. Electron. 10 (2009) 1307.

[8] D. Heredia, L. Fernandez, L. Otero, M. Ichikawa, C-Y. Lin, Y-L. Liao, S-A. Wang, K-T. Wong, F. Fungo. J. Phys. Chem. C 115 (2011) 21907.

[9] M.I. Mangione, R.A. Spanevello, A. Rumbero, D. Heredia, G. Marzari, L. Fernandez, L. Otero, F. Fungo. Macromolecules 46 (2013) 4754.

[10] B. Lüssem, M. Riede, K. Leo. Phys. Status Solidi A-Appl. Mat. 210 (2013) 9.

[11] S.D. Dimitrov, J.R. Durrant. Chem. Mat. 26 (2014) 616.

[12] M. Wright, A. Uddin. Sol. Energy Mater. Sol. Cells. 107 (2012) 87.

[13] S-S Li, C-W. Chen. J. Mat. Chem. A 1 (2013) 10574.

[14] P. Brown, P. Kamat. J. Am. Chem. Soc. 130 (2008) 8890.

[15] S. Günes, N.S. Sariciftci. Inorg. Chim. Acta 361 (2008) 581.

[16] B.P. Nguyen, T. Kim, C.R.J. Park. J. Nanomater. 2014 (2014) Art. ID 243041.

[17] A.L. Rogach. Semiconductor Nanocrystal Quantum Dots: Synthesis, Assembly, Spectroscopy and Applications; Springer: Wien, New York, 2008.

[18] J.H. Bang, P.V. Kamat. ACS Nano 3 (2009) 1467.

[19] L. Zhao, Z. Lin. Adv. Mater. 24 (2012) 4353.

[20] I. Mora-Seró, S. Giménez, F. Fabregat-Santiago, R. Gómez, Q. Shen, T. Toyoda, J. Bisquert. J. Acc. Chem. Res. 42 (2009) 1848.

[21] L. Etgar. Materials 6 (2013) 445.

[22] S. Dayal, N. Kopidakis, D.C. Olson, D.S. Ginley, G. Rumbles. Nano Lett. 10 (2010) 239.

[23] Y-L Lee, Y-S. Lo. Adv. Funct. Mater. 19(2009) 604.

[24] E. Zillner, J. Kavalakkatt, B. Eckhardt, T. Dittrich, A. Ennaoui, M. Lux-Steiner. Thin Solid Films 520 (2012) 5500.

[25] J.N. De Freitas, I.R. Grova, L.C. Akcelrud, E. Arici, N.S. Sariciftci, A.F.J. Nogueira. Mater. Chem. 20 (2010) 4845.

[26] J. Lim, D. Lee, M. Park, J. Song, S. Lee, :S. Kang, C. Lee, K.J. Char. J. Phys. Chem. C. 118 (2014) 3942.

[27] J.Y. Lek, L. Xi, B.E. Kardynal, L.H. Wong, Y.M. Lam. ACS Appl. Mater. Interf., 3 (2011) 287.

[28] M. Li, S. Tang, F. Shen, M. Liu, F. Li, P. Lu, D. Lu, M. Hanif, Y.J. Ma. Electrochem. Soc. 155 (2008) H287–H291.

[29] C. Gu, T. Fei, M. Zhang, C. Li, D. Lu, Y. Ma. Electrochem. Commun. 12 (2010) 553.

[30] M. Gervaldo, M. Funes, J. Durantini, L. Fernandez, F. Fungo, L. Otero. Electrochim. Acta 55 (2010) 1948.

[31] P.A. Liddell, M. Gervaldo, J.W. Bridgewater, A.E. Keirstead, S. Lin, T.A. Moore, A.L. Moore, D. Gust. Chem. Mater. 20 (2008) 135.

[32] Y. Shi, S-C. Luo, W. Fang, K. Zhang, E.M. Ali, F.Y.C. Boey, J.Y. Ying, J. Wang, H-H. Yu, L-J. Li. Organic Electronics 9 (2008) 859.

[33] N.K. Subbaiyan, I. Obraztsov, C.A. Wijesinghe, K. Tran, W. Kutner, F. D'Souza. F. J. Phys. Chem. C 113 (2009) 8982.

[34] Th.Dittrich, S. Bönisch, P. Zabel, S. Dube. Rev. Sci. Instrum. 79 (2008) 113903 (1-6).

[35] A. Boulesbaa, A. Issac, D. Stockwell, Z. Huang, J. Huang, J. Guo, T.J. Lian. J. Am. Chem. Soc. 129 (2007) 15132.

[36] V. Palermo, G. Ridolfi, A.M. Talarico, L. Favaretto, G. Barbarella, N. Camaioni, P. Samorì. Adv. Funct. Mater. 17 (2007) 472.

[37] E. Zillner, T. Dittrich. Phys. Status Solidi-Rapid Res. Lett. 5 (2011) 256.

[38] E.N. Durantini. Synth. Commun. 29 (1999) 4201.

[39] J. Averdung, J. Mattay, D. Jacobi, W. Abraham. Tetrahedron 51 (1995) 2543.

[40] M. Prato, Q.C. Li, F. Wudl, V. Lucchini. J. Am. Chem. Soc. 115 (1993) 1148.

[41] A. Yashiro, Y. Nishida, M. Ohno, S. Eguchi, K Kobayashi. Tetrahedron Lett., 39 (1998) 9031.

[42] L. Groenendaal, G. Zotti, P.H. Aubert, S.M. Waybright, J.R. Reynolds. Adv. Mater. 15 (2003) 855.

[43] L. Groenendaal, F. Jonas, D. Freitag, H. Pielartzik, J.R. Reynolds. Adv. Mater., 12 (2000) 481.

[44] L. Echegoyen, L.E. Echegoyen. Acc. Chem. Res. 31 (1998) 593.

[45] C.A. Reed, R.D. Bolskar. Chem. Rev. 100 (2000) 1075.

[46] A. Hirsch, M. Brettreich. Fullerenes: Chemistry and Reactions; Wiley-VCH: Erlangen, Germany, 2005.

[47] T. Yamazaki, Y. Murata, K. Komatsu, K. Furukawa, M. Morita, N. Maruyama, T. Yamao, S. Fujita. Org. Lett. 6 (2004) 4865.

[48] a) J.L. Segura, R. Gómez, R. Blanco, E. Reinold, P. Bäuerle. Chem. Mater. 18 (2006) 2834. b) T. Darmanin, F. Guittard. ChemPhysChem. 14 (2013) 2529.

[49] J. Natera, L. Otero, L. Sereno, F. Fungo, N-S. Wang, Y-M. Tsai, T-Y. Hwu, K-T. Wong. Macromol. 40 (2007) 4456.

[50] A. Yashiro, Y. Nishida, M. Ohno, S. Eguchi, K. Kobayashi. Tetrahedron Lett., 39 (1998) 9031.

[51] J. Averdung, J. Mattay, D. Jacobi, W. Abraham. Tetrahedron 51 (1995) 2543.

[52] A. Cravino, G. Zerza, H. Neugebauer, M. Maggini, S. Bucella, E. Menna, M. Svensson, M. R. Andersson, C. J. Brabec, N. S. Sariciftci. J. Phys. Chem. B 106 (2002) 70.

[53] H. Imahori, S. Kitaura, A. Kira, H. Hayashi, M. Nishi, K. Hirao, S. Isoda, M. Tsujimoto, M. Takano, Z. Zhe, Y. Miyato, K. Noda, K. Matsushige, K. Stranius, N. V. Tkachenko, H. Lemmetyinen, L. Qin, S. J. Hurst, C. A. Mirkin. J. Phys. Chem. Lett. 3 (2012) 478.

[54] P. Piotrowski, K. Zarebska, M. Skompska, A. Kaima. Electrochimica Acta 148 (2014) 145.

[55] M. Czichy, P. Wagner, L. Grzadziel, M. Krzywiecki, A. Szwajca, M. Łapkowski, J. Zaka, D.L. Officer. Electrochimica Acta 141 (2014) 51.

[56] L. Kronik, Y. Shapira. Surf. Sci. Rep. 37 (1999) 1.

[57] V. Duzhko, V.Y. Timushenko, F. Koch, T. Dittrich. Phys. Rev. B. 64 (2001) 075204.

[58] L. Kronik, Y. Shapira. Surf. Interface Anal. 31 (2001) 954.

[59] J. Durantini, G. Morales, M. Santo, M. Funes, E. Durantini, F. Fungo, T. Dittrich, L. Otero, M. Gervaldo. Org. Electron. 13 (2012) 604.

[60] D. Heredia, L. Otero, M. Gervaldo, F. Fungo, T. Dittrich, C-Y. Lin, L-C. Chi, F-C. Fang, K-T. Wong, K.-T. Thin Solid Films 527 (2013) 175.

[61] M. Amelia, C. Lincheneau, S. Silvi, A. Credi. Chem. Soc. Rev. 41 (2012) 5728.

[62] M.N. Berberan-Santos, E.N. Bodunov, B. Valeur. Chem. Phys. 315 (2005) 171.

[63] S. Fengler, E. Zillner, T. Dittrich. J. Phys. Chem. C 117 (2013) 6462.

[64] E. Zillner, S. Fengler, P. Niyamakom, F. Rauscher, K. Koehler, T. Dittrich. J. Phys. Chem. C 116 (2012) 16747.

[65] E.-K. Park, J.-H. Kim, I.A. Ji, H. M. Choi, J.-H. Kim, K.-T. Lim, J. H. Bang, Y.-S. Kim. Microelectronic Engineering 119 (2014) 169.

[66] J.N. de Freitas, I.R. Grova, L.C. Akcelrud, E. Arici, N.S. Sariciftci, A. F. Nogueira. J. Mater. Chem. 20 (2010) 4845.

[67] S. Ananthakumar , J. Ramkumar , S. Moorthy Babu. Materials Science in Semiconductor Processing 22 (2014) 44.

[68] Jingyang Wang, Tianjin Zhang, Duofa Wang, Ruikun Pan, Qingqing Wang, Hanming Xia. Chem. Phys. Letters 541 (2012) 105.

[69] Shailesh N. Sharma , Tanvi Vats , N. Dhenadhayalan , P. Ramamurthy , A.K. Narula. Solar Energy Materials & Solar Cells 100 (2012) 6.

[70] Ruchuan Liu. Materials 2014, 7, 2747.

Figure captions

Figure 1: Chemical structure and synthesis scheme of EDOT-C_{60} monomers.

Figure 2: a) Repetitive cyclic voltammograms of a 1.0 mM solution of EDOT-C_{60} in *o*-DCB with 0.1 M of TBATFB. Thick black line denotes the first CV. b) Cyclic voltammogram of a PEDOT-C_{60} film electro-deposited on a gold electrode in *o*-DCB with 0.1 M of TBATFB. The scan rates were 100 mV/s.

Figure 3: a) Electronic absorption spectrum of EDOT-C_{60} monomer in DCM. b) Diffuse reflectance spectrum of PEDOT-C_{60} film on ITO. The picture shows the PEDOT-C_{60}/ITO modified electrode analyzed.

Figure 4: 3D model of PEDOT-C_{60} polymer optimized by MM+ calculation at HyperChem software.

Figure 5: Cross section of a PEDOT-C_{60} layer electro-polymerized within 10 cycles on a glass/Cr/Au substrate. The insert shows the sample with the coated area.

Figure 6: PEDOT film thicknesses in function of the number of potential scan cycles. The insert shows measurement done with the step profiler for 2 and 10 scan cycles.

Figure 7: SPV transients of CdSe-QDs/Au (circles), CdSe-QDs/PEDOT/Au (triangles) and CdSe-QDs/PEDOT-C_{60}/Au (stars). λ_{exc} = 590 nm (2.1 eV). The arrow marks the time at which the laser pulse was switched on. PEDOT and PEDOT-C_{60} film thickness ~ 125 nm.

Figure 8: Scheme of local separation of photo-generated charge carriers for CdSe-QDs/Au (a), CdSe-QDs/PEDOT (b) and CdSe-QDs/PEDOT-C_{60} (c).

Figure 9: In phase (thick red lines) and phase-shifted 90^{o} (thin black lines) SPV spectra for CdSe-QDs on an un-treated gold electrode (a), PEDOT decorated with CdSe-QDs (b), PEDOT-C_{60} (c) and PEDOT-C_{60} decorated with CdSe-QDs (d). [note that in order to facilitate the comparison the actual SPV amplitudes are enlarged ten times in (b) and (c) figures, and two times in (a)]. PEDOT and PEDOT-C_{60} films thickness ~ 125 nm.

Figure 1

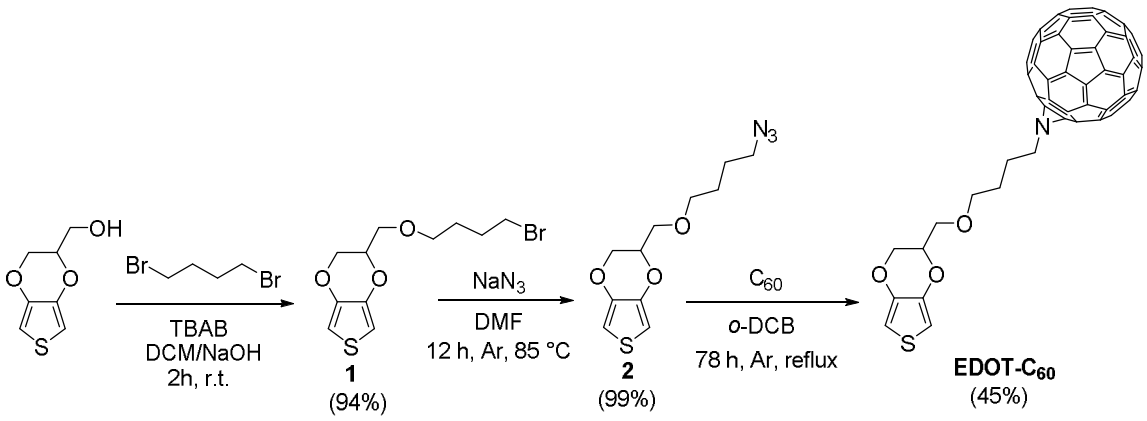

Figure 2

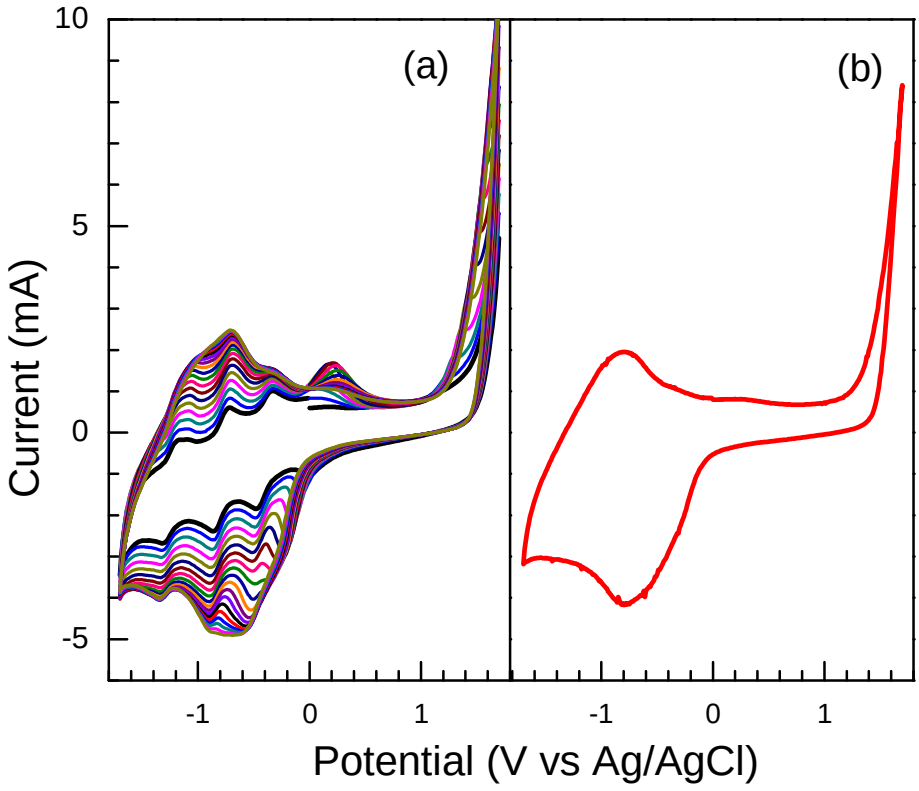

Figure 3

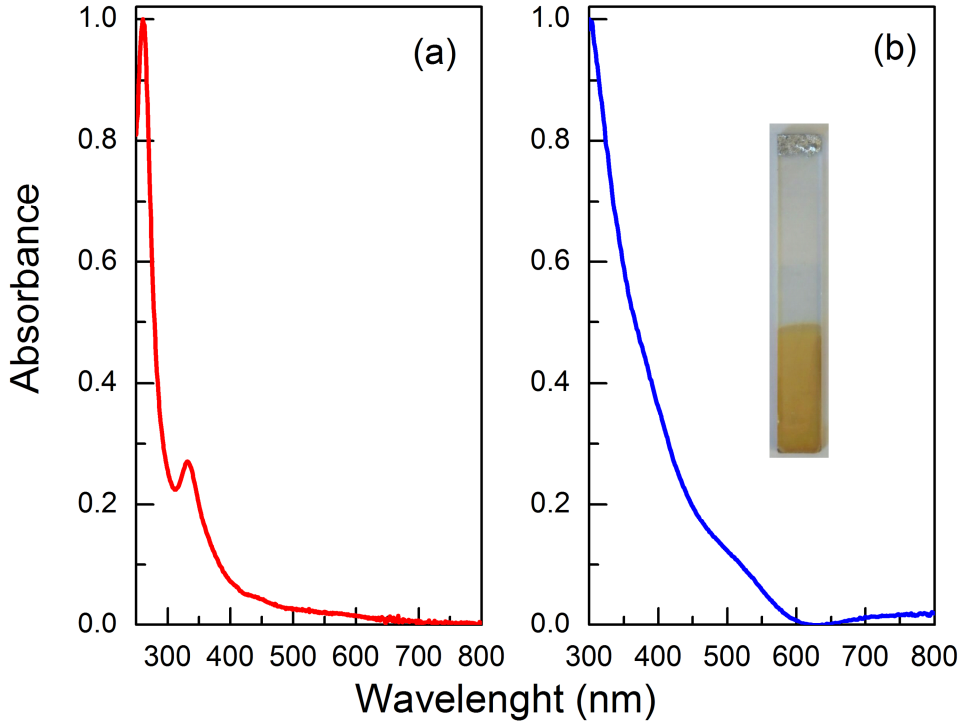

Figure 4

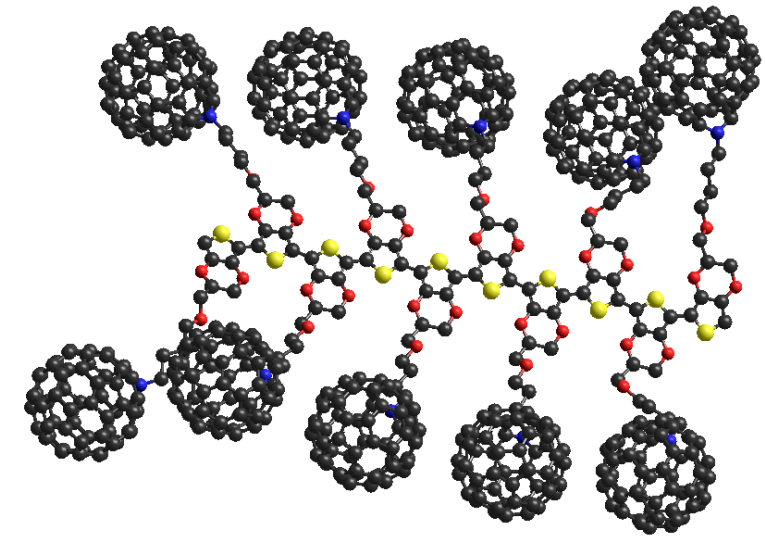

Figure 5

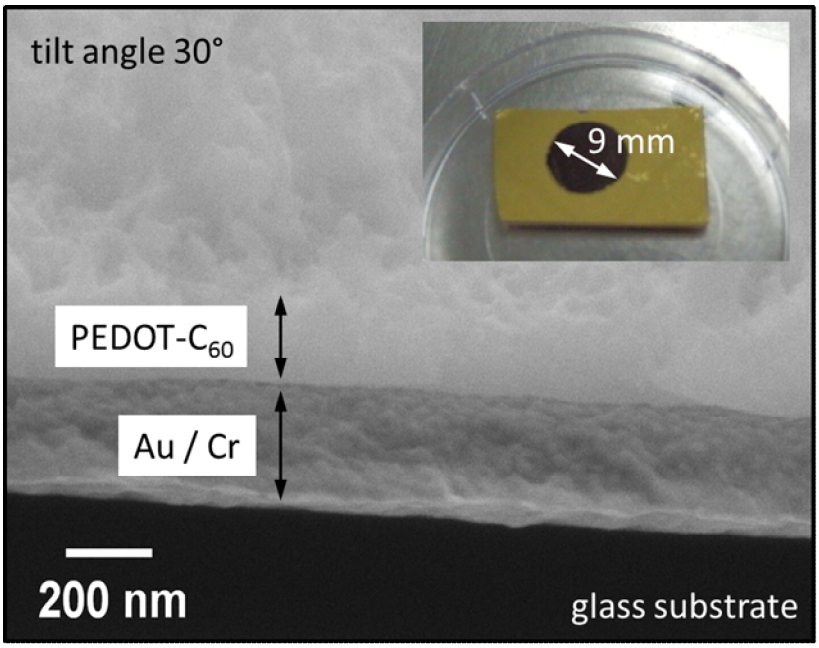

Figure 6

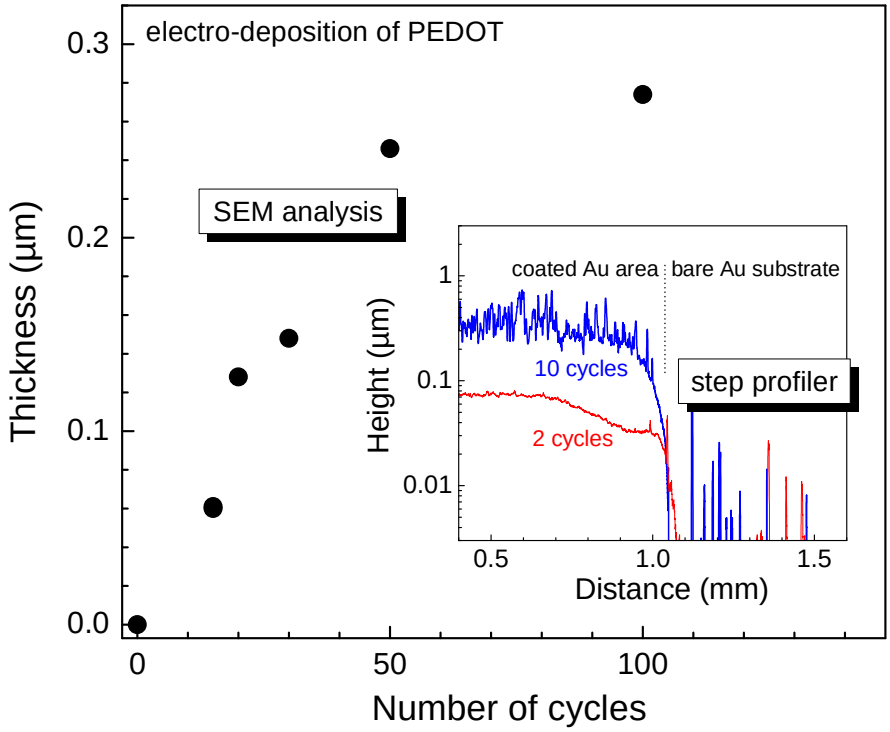

Figure 7

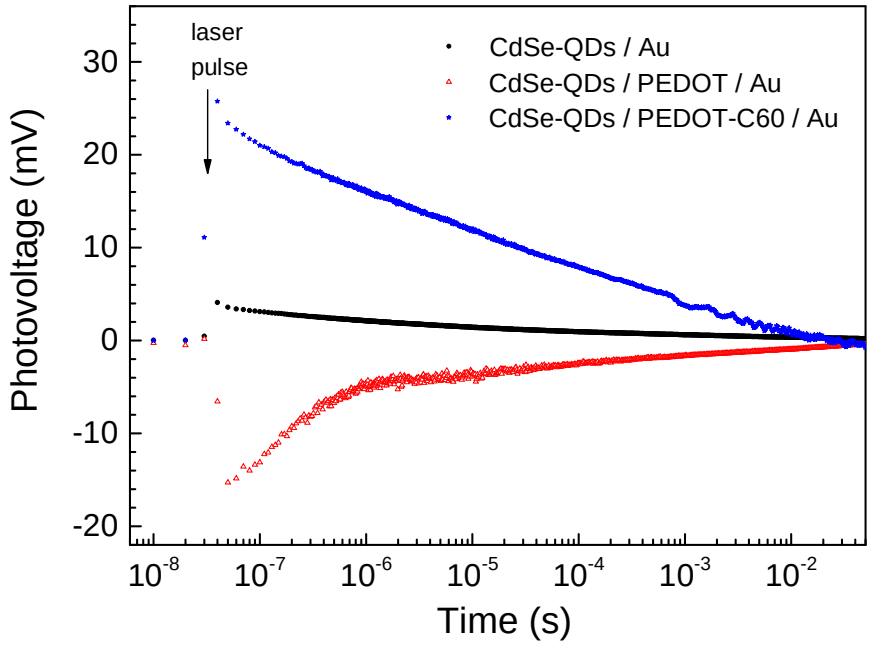

Figure 8

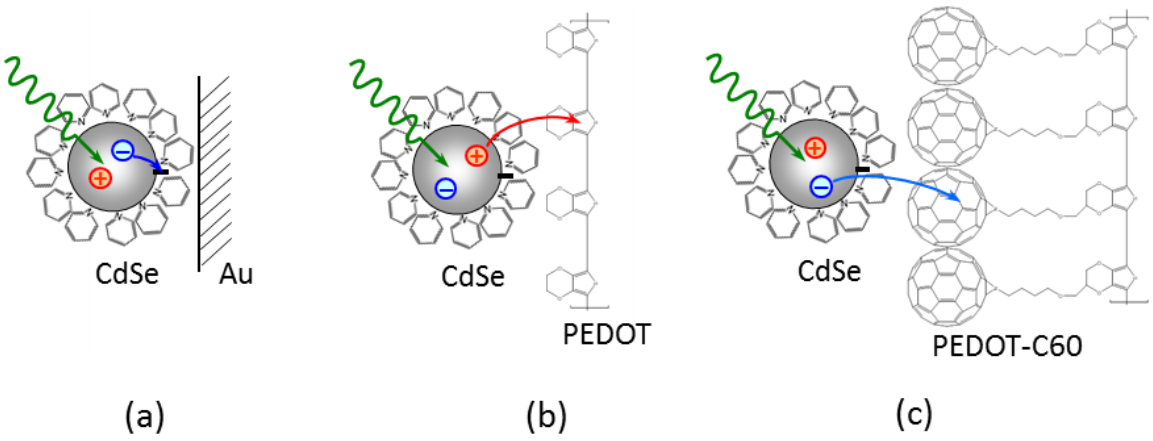

Figure 9